JPET Fast Forward. Published on May 25, 2006 as DOI: 10.1124/jpet.106.104737

Pharmacology of 2-[4-(4-chloro-2-fluorophenoxy)phenyl]-pyrimidine-4-carboxamide (PPPA): a potent, broad-spectrum state-dependent sodium channel blocker for treating pain states

Victor I. Ilyin, James D. Pomonis, Garth T. Whiteside, James E. Harrison, Michelle S. Pearson, Lilly Mark, Paul I. Turchin, Susan Gottshall, Richard B. Carter, Phong Nguyen, Derk J. Hogenkamp, Shakira Olanrewaju, Elfrida Benjamin and Richard M. Woodward

Discovery Research, Purdue Pharma LP, 6 Cedar Brook Drive, Cranbury, NJ 08512-3612, USA (V.I.I.)

JPET Fast Forward. Published on May 25, 2006 as DOI: 10.1124/jpet.106.104737
This article has not been copyedited and formatted. The final version may differ from this version.

Running title page: PPPA - Na^+ channel blocker for treating pain

Corresponding author: Victor I. Ilyin, 6 Cedar Brook Drive, Cranbury, NJ 08512, Tel (609) 409-5874; Fax (609) 409-6922; E-mail: victor.ilyin@pharma.com

Number of pages: 44

Number of tables: 4

Number of figures: 5

Number of references: 39

Number of words in Abstract: 247

Number of words in Introduction: 591

Number of words in Discussion: 1470

Abbreviations: CBZ, carbamazepine; CNS, central nervous system; CSF, cerebro-spinal fluid; DRG, dorsal root ganglion; FCA, Freund's complete adjuvant; HEK, human embryonic kidney; I_{Na}, sodium current; i.p., intraperitoneal; K_I, dissociation constant for the inactivated channel state; K_R, dissociation constant for the resting state; k_+, pseudo-first order rate constant (for binding to inactivated channels); LTG, lamotrigine; MAD, minimum ataxic dose; MED, minimum effective dose; PNS, peripheral nervous system; p.o., oral gavage; PPPA, 2-[4-(4-chloro-2-fluorophenoxy)phenyl]-pyrimidine-4-carboxamide; PSN, partial spinal nerve ligation; PWT, paw withdrawal threshold; $rNa_v1.2$, rat brain type IIa Na^+ channel; s.c., subcutaneous; TI, therapeutic index, TTX, tetrodotoxin; TTX-R, tetrodotoxin-resistant; TTX-S, tetrodotoxin-sensitive; τ_{repr}, time constant of repriming.

Recommended section assignment: Neuropharmacology

JPET Fast Forward. Published on May 25, 2006 as DOI: 10.1124/jpet.106.104737
This article has not been copyedited and formatted. The final version may differ from this version.

ABSTRACT

Voltage-gated Na^+ channels play important roles in establishing pathological neuronal hyperexcitability associated with chronic pain in humans. Na^+ channel blockers, such as carbamazepine (CBZ) and lamotrigine (LTG), are efficacious in treating neuropathic pain, however their therapeutic utility is compromised by CNS side effects. We reasoned that it may be possible to gain superior control over pain states, and in particular a better therapeutic index, by designing broad-spectrum Na^+ channel blockers with higher potency, faster onset kinetics and greater levels of state-dependence than existing drugs. 2-[4-(4-Chloro-2-fluorophenoxy)phenyl]-pyrimidine-4-carboxamide (PPPA) is a novel structural analogue of the state-dependent Na^+ channel blocker V102862 (4-(4-fluorophenoxy)benzaldehyde semicarbazone). Tested on recombinant rat $Na_v1.2$ channels and native Na^+ currents in cultured rat dorsal root ganglion neurons, PPPA was approximately 1000-times more potent, had 2000-fold faster binding kinetics and $\geq$10-fold higher levels of state-dependence than CBZ and LTG. Tested in rat pain models against mechanical endpoints, PPPA had minimal effective doses of 1-3 mg/kg p.o. in partial sciatic nerve ligation, Freund's complete adjuvant, and post-incisional pain. In all cases, efficacy was similar to clinically relevant comparators. Importantly, PPPA did not produce motor deficits in the accelerating rotarod assay of ataxia at doses up to 30 mg/kg p.o., indicating a therapeutic index >10, which was superior to CBZ and LTG. Our experiments suggest that high potency, broad-spectrum state-dependent Na^+ channel blockers will have clinical utility for treating neuropathic, inflammatory and post-surgical pain. Optimizing the biophysical parameters of broad-spectrum voltage-gated Na^+ channel blockers may lead to improved pain therapeutics.

INTRODUCTION

Voltage-gated Na^+ channels are comprised of α and β subunits co-associated with various ancillary proteins (Catterall, 2000; Chahine et al., 2005). In mammals, there are nine cloned isoforms of α subunit with functional activity and four isoforms of β subunit (Goldin, 2001). The α subunits ($Na_v1.1$-9) form voltage-gated Na^+ channels, containing the ion pore and voltage sensor (Scheuer et al., 1990; Goldin, 2001). The β subunits (β1-4) modulate channel biophysics and regulate channel expression and localization (Isom, 2001; Chahine et al., 2005). Na^+ channel α subunits have differential localization and distinct biophysical properties, suggesting that different subtypes of Na^+ channel have been tailored through evolution to perform tissue- and neuron-specific functions (Scheuer et al., 1990; Catterall, 2000; Goldin, 2001).

Multiple lines of evidence now implicate voltage-gated Na^+ channels in establishing and maintaining patterns of pathological neuronal excitability that underlie chronic pain states. For example: (i) Nerve injury and inflammation cause changes in the levels of expression and distribution of Na^+ channel α subunits and β subunits in primary afferent neurons, leading to changes in action potential parameters and firing patterns (e.g. Waxman et al., 2000; Coward et al., 2000; Craner et al., 2002; Takahashi et al., 2003; Coggeshall et al., 2004; Hong et al., 2004; Lai et al., 2004). (ii) Neuronal hyperexcitability is associated with functional modulation of Na^+ channels by signal transduction cascades (Lai et al., 2004; Chahine et al., 2005). (iii) Blocking and reversing changes in Na^+ channel expression in dorsal root ganglion (DRG) in vivo reduces hypersensitivity in animal pain models (Lai et al., 2002; Gold et al., 2003; Hains et al., 2004). (iv) Mice with selective Na^+ channel α subunits genetically knocked-out show reduced sensitivity in pain models. In particular, $Na_v1.8$-null mice demonstrate altered thresholds to mechanical and thermal stimuli as compared to wild-type and show deficits in visceral pain (Akopian et al., 1999; Laird et al., 2002). While $Na_v1.7$ knock-out mice have substantially reduced sensitivity to

mechanical and thermal stimuli in models of inflammatory pain (Nassar et al., 2004; Nassar et al., 2005).

It is therefore not surprising that drugs with Na^+ channel blocking activity, such as carbamazepine (CBZ), lamotrigine (LTG), mexiletine and lidocaine, show efficacy in animal pain models (Hunter et al., 1997; Kiguchi et al., 2004; De Vry et al., 2004) and, moreover, have utility in treating pain states in humans (e.g. Mao and Chen, 2000; Jensen, 2002; Petersen et al., 2003). However, these drugs were developed as anticonvulsants, anti-arrhythmics and anesthetics, with no attempt to optimize the Na^+ channel blocking activity for treating chronic pain. And in general, the therapeutic utility of these agents is compromised by dose limiting side effects, particularly sedation, headache, dizziness and motor disturbances (ibid).

2-[4-(4-Chloro-2-fluorophenoxy)phenyl]-pyrimidine-4-carboxamide (PPPA) (figure 1, insert) is a novel structural analogue of the state-dependent Na^+ channel blocker 4-(4-fluorophenoxy)benzaldehyde semicarbazone (V102862 / Co 102862) (Dimmock et al., 1996; Ilyin et al., 2005). PPPA was discovered as part of a systematic exploration of V102862 analogues where the phenoxyphenyl portion of the molecule was fixed and the semicarbazone moiety was substituted by various heterocycles. The goal of the research was to design Na^+ channel blockers with higher in vitro potency, faster binding kinetics and more pronounced levels of state-dependence compared to existing drugs. The Na^+ channel subtype-selectivity of these compounds was consistently <10-fold (V.I. Ilyin, unpublished data). Selected compounds were profiled in rat pain models to see if altering the biophysics of inhibition at the molecular level translated into improved potency, efficacy and side effects compared to clinically relevant drugs. In the current paper we report the data for PPPA.

METHODS

Materials and reagents were purchased from Sigma-Aldrich Company (St. Louis, MO) unless otherwise noted.

MOLECULAR BIOLOGY

A cell line expressing $rNa_v1.2$ channels was constructed using conventional methods. Briefly, the plasmid pCMV-RIIA, which encodes the rat type IIa Na^+ channel under control of the CMV promoter, was obtained from Dr. Alan Goldin, University of California, Irvine, CA. Bacterial growth, DNA preparations and restriction enzyme characterizations were performed using standard procedures. HEK-293 cells were plated at a density of 3×10^5 cells $well^{-1}$ in a 6 well plate and transfected the following day with pCMV-RIIA DNA using Transfast reagent (Promega Inc., Madison, WI). After 3 weeks of selection in 400 μg ml^{-1} G418, resistant colonies were isolated, expanded and characterized by electrophysiological analysis. Several clones expressing tetrodotoxin-sensitive (TTX-S) inward currents were identified. Clone B2 (NaIIA-B2), with mean current densities of $\geq$250 pA/pF, was expanded and further electrophysiological analyses performed. The currents were completely blocked by 400 nM TTX and reversed at the predicted equilibrium potential for Na^+: 65 $\pm$ 2 mV (n=15). The data indicate that the currents were due to activation of voltage-gated Na^+ channels. Untransfected cells displayed small ($\leq$10 pA/pF) and variable inward currents that were only partially blocked by 1μM TTX.

ELECTROPHYSIOLOGY

Cell preparation

HEK-293 cells. HEK-293 cells were cultured using standard techniques (Ilyin et al., 2005). For electrophysiology, cells were plated onto 35 mm Petri dishes pre-coated with poly-D-lysine

(PDL), at a density of 2-4 x 10^4 cells $dish^{-1}$ on the day of re-seeding from confluent cultures. HEK-293 cells were suitable for recordings for 3-4 days after plating.

Isolation and acute culture of rat DRG neurons Acutely dissociated DRG neurons were prepared from newborn (3-8 days postnatal) Sprague Dawley (Charles River) rats using a modification of published procedures (Rush et al., 1998). Briefly, pups were anaesthetized on ice and sacrificed by rapid decapitation. DRG were dissected out in cold calcium- and magnesium-free Hanks buffer (CMF, Gibco), trimmed, and incubated for 90 min at 35° C in 0.3 mg/mL collagenase in Krebs buffer (in mM: 120 NaCl, 5 KCl, 1.8 $CaCl_2$, 1 $MgCl_2$, 5 HEPES, 25 d-glucose, pH 7.4). Ganglia were rinsed in CMF at room temperature and incubated for 30 min at 35° C in 2.5 mg/mL trypsin in CMF, then rinsed with Krebs buffer at room temperature, and triturized using fire-polished Pasteur pipettes. Liberated cells were plated on PDL pre-coated 35 mm plastic Petri dishes in Krebs buffer. Cells were suitable for electrophysiological recordings for up to 2 weeks.

Whole cell patch-clamp recordings

Whole-cell voltage-clamp recordings were made using standard patch-clamp technique at room temperature (~22°C). Currents were recorded using an Axopatch 200A amplifier (Axon Instruments, Union City, CA) and were leak-subtracted (P/4 or by the built-in analog circuitry), low-pass filtered (3 kHz, 8-pole Bessel), digitized (20-50-μs intervals), and stored using Digidata 1200 B interface and Pclamp8/Clampex software (Axon Instruments, Union City, CA). The patch-clamp pipettes were pulled from WPI, thick-walled borosilicate glass (WPI, Sarasota, FL). The pipette resistances ranged from 1.5 to 3 MΩ. Residual series access resistance was in the range of 0.5-1.2 MΩ after partial (75-80%) cancellation using built-in amplifier circuitry. In the recording chamber, cells were continuously superfused at a speed of ~1 mL min^{-1} with physiological saline solution.

Solutions and drug application

Hek-293 cells The external solution for NaIIA-B2 (HEK-293) cells contained (in mM): 150 NaCl, 5.4 KCl, 1.8 $CaCl_2$, 1 $MgCl_2$, 10 d-glucose, 5 HEPES; pH 7.4 (NaOH). The internal solution contained (in mM): 130 CsF, 20 NaCl, 1 $CaCl_2$, 2 $MgCl_2$, 10 EGTA, 10 HEPES, pH 7.4 (CsOH); osmolality set at ~10 mOsmol kg^{-1} lower than that for the external solution.

Rat DRG neurons Small (<25 μm) and medium (25-40 μm) neurons were used for assaying compounds on fast TTX-S and slow tetrodotoxin-resistant (TTX-R) Na^+ currents. External solution was (in mM): 65 NaCl, 5 KCl, 50 choline chloride, 1.8 $CaCl_2$, 1 $MgCl_2$, 5 d-glucose, 5 HEPES, 5 HEPES Na^+ salt, 20 TEA chloride; pH 7.4 (NaOH). The internal solution had the same ionic content as that used for HEK-293 cell recordings. Osmolality was set by ~5 mOsmol kg^{-1} lower than that for the bathing solution.

Drug solutions and intervening intervals of wash were applied through a linear array of flow pipes (Drummond Microcaps, 2-μl, 64-mm length) producing full solution exchange within a few hundred ms. PPPA, lamotrigine (LTG) and carbamazepine (CBZ) were dissolved in dimethylsulfoxide (DMSO) and then diluted in DMSO to make 0.3-200 mM stock solutions. The stock solutions were diluted into external solution on each day of experimentation to generate final concentrations of 0.003-200 μM. At the highest concentration (200 μM for LTG and CBZ) the concentration of DMSO was 0.2%. In these experiments, data was corrected for a minor inhibition caused by the vehicle. CBZ was from RBI (Natick, MA) and LTG was synthesized in-house. PPPA was synthesized as described in issued US patent (Hogenkamp et al., 2005).

Protocols and data analysis

The voltage pulse protocols and procedures used to measure the state-dependent block of voltage-gated Na channels were described in detail in a previous article (Ilyin et al., 2005).

JPET Fast Forward. Published on May 25, 2006 as DOI: 10.1124/jpet.106.104737
This article has not been copyedited and formatted. The final version may differ from this version.

Some adjustments were made to allow for kinetic differences. Data are presented as mean ± standard error (n = number of experiments) with statistical significance assessed with paired *t*-tests. The level of significance was set at $P < 0.05$.

FLUORESCENCE PLATE READER (FLIPR) MEASUREMENTS

FLIPR calcium mobilization assay for IMR-32 cells

PPPA was profiled in human neuroblastoma IMR-32 cells expressing significant proportion of N-type Ca^{2+} channels. The channels were opened by addition of KCl, and Ca^{2+} mobilization was measured by fluo-4 fluorescence on Fluorimetric Imaging Plate Reader ($FLIPR^{96}$, Molecular Devices, Inc., Sunnyvale, CA).

The assay is described in detail elsewhere (Benjamin et al., 2006). In brief, one day prior to performing this assay, IMR-32 cells were seeded on poly-D-lysine-coated 96-well clear-bottom black plates (Becton Dickinson, Franklin Lakes, NJ) at 75,000 cells/well. On the day of the assay, the cell plates were washed with assay buffer (127 mM NaCl, 1 mM KCl, 2 mM $MgCl_2$, 700 µM NaH_2PO_4, 5 mM $CaCl_2$, 5 mM $NaHCO_3$, 8 mM HEPES, 10 mM glucose, pH 7.4), Cells were loaded with 0.1 mL of assay buffer containing 20 µM nifedipine and 6 µM fluo-4-AM for 1 hr at 37°C. Cells were then washed once with 0.1 mL assay buffer containing 20 µM nifedipine, then replaced with 0.05 ml of the same. Plates were transferred to the $FLIPR^{96}$. Basal fluo-4 fluorescence was measured for 15 sec, then 0.05 mL of each compound diluted at a 4x concentration in assay buffer was added, and fluorescence was read for another 5 min. Then 0.1 mL KCl dissolved in assay buffer was added and fluorescence measured for another 45 sec. Final test compound concentrations on the cells after FLIPR read ranged from about 1 nM to about 20 µM (10 pM to 20 µM for ω-conotoxin (ω-ctx) MVIIA, positive control), final nifedipine concentration was 5 µM, and final KCl concentration was 90 mM. Final DMSO concentration

was held constant at 0.5%. Data were collected over the entire time course of the FLIPR read and then analyzed using Graph Pad Prism (version 3.02, Graph Pad, San Diego, CA) software.

Data analysis

Experiments were expressed as percentage of control. This refers to the average of multiple determinations normalized to the maximum average counts in the presence of 90 mM KCl and to the minimum average counts in the presence of 50 nM ω-ctx MVIIA block of 90 mM KCl. Normalization calculations were conducted using GraphPad Prism software or Microsoft Excel. Theoretical curves were generated using nonlinear regression curve-fitting analysis in GraphPad Prism software.

IN-VIVO PHARMACOLOGY

Compounds, animals and general procedures

For all in-vivo pharmacological studies, PPPA was administered by oral gavage (p.o.) as a suspension in 0.5% methylcellulose dissolved in distilled water. The mu opioid receptor agonist morphine was dissolved in 0.9% saline solution and administered subcutaneously (s.c.). The anticonvulsant gabapentin (Kemprotec; Middlesborough, UK) was dissolved in 0.9% saline and administered by intraperitoneal (i.p.) injection. The cycloxogenase-2 inhibitor celecoxib (Toronto Research Chemicals; Toronto, Canada), the nonsteroidal anti-inflammatory drug indomethacin, and the anticonvulsant CBZ were suspended in 0.5% methyl-cellulose and administered orally (p.o.). The anticonvulsant LTG was dissolved in 25% hydroxypropyl-β-cyclodextrin and administered via intraperiotoneal (i.p.) injection. The Purdue Institutional Animal Care and Use Committee approved all animal procedures according to the guidelines of the Office of Laboratory Animal Welfare. Male Sprague-Dawley rats (Taconic) weighing 90 to110 g at the

start of nerve ligation experiments or 180 to 200 g at the start of acute, inflammatory, incisional and rotarod experiments, were used. Animals were group-housed and had free access to food and water at all times, except prior to oral administration of drugs when food was removed $\geq$12 h before dosing. For comparison with compound-treated groups, animals treated with appropriate drug vehicle were included in each experiment. The volume of administration and all other experimental procedures and conditions for vehicle and compound-treated rats were identical. All experiments were blinded to behavioral testers through use of randomization codes.

Post-surgical hyperalgesia

The effect of PPPA on post-surgical pain was assessed using an incisional pain model, as described previously by Brennan et al. (1996). Hind paw withdrawal thresholds (PWT) to a noxious mechanical stimulus were determined using a model 7200 analgesymeter (Ugo Basile; Varese, Italy). Cut-off was set at 250 g and the endpoint was taken as complete paw withdrawal. PWT was determined once for each rat at each time point. Baseline PWTs were determined and a 1 cm longitudinal incision was made through skin and fascia of the plantar aspect of the paw. Unoperated rats served as controls. Twenty-four hours following plantar incision, pre-drug PWTs were measured and the rats (n = 9-20/group) received a single dose of either 3, 10 or 30 mg/kg p.o. PPPA, 30 mg/kg p.o. celecoxib or vehicle. PWTs were determined again 1, 3, 5 and 24 h post drug administration. Percent reversal of hyperalgesia for each animal was defined by equation 1:

(1) $$\%\ reversal = \frac{Postdose\ threshold - predose\ threshold}{Baseline\ threshold - predose\ threshold}\ x\ 100$$

Hyperalgesia due to nerve injury

The partial sciatic nerve ligation model (PSN) was used as a model of nerve injury-related pain in rats, as described previously by Seltzer et al. (1990). PWTs to a noxious mechanical stimulus were determined as described above. Baseline PWTs were determined and partial ligation of the left sciatic nerve was performed under isofluorane (2% in oxygen) inhalation anesthesia. Three weeks following nerve ligation, pre-drug PWTs were measured and the rats received a single dose of either 3, 10, or 30 mg/kg p.o. PPPA, 100 mg/kg i.p. gabapentin or vehicle. PWT was again determined 1, 3, 5 and 24 h post drug administration. In separate experiments, the potency and efficacy of CBZ and LTG were examined using doses of 30, 100, and 300 mg/kg p.o. for CBZ and 10, 30 and 100 mg/kg i.p. for LTG. In both cases, 100 mg/kg i.p. gabapentin served as the positive control.

Inflammatory hyperalgesia

The efficacy of PPPA against hyperalgesia associated with inflammation was investigated using the Freund's complete adjuvant (FCA) model in rats. PWTs to a noxious mechanical stimulus were determined as described above. Baseline PWT was determined, the rats (n = 8-28/group) were anesthetised with isofluorane (2% in oxygen) and received an intraplantar injection of 50% FCA (50 μL diluted in 0.9% saline) to the left hind paw. Twenty-four hours following FCA injection, pre-drug PWT's were measured and the rats received a single dose of either 1, 3, or 10 mg/kg p.o. PPPA, 30 mg/kg p.o. celocoxib (the positive control) or vehicle (i.p. volume = 2 mL/kg). PWT was again determined 1, 3, 5 and 24 h post drug administration.

The rotarod assay of ataxia/motor coordination

To assess effects of PPPA, CBZ and LTG on motor performance, rats were tested using the accelerating rotarod (Accuscan; Columbus, OH). The rotarod was set to accelerate from 4 to 40 rpm over 300 seconds with the maximum time spent on the rotarod set at 300 seconds. Rats (n = 10/group) received two training trials on the first day and then received a single dose of either

3, 10, or 30 mg/kg p.o. PPPA, 100 mg/kg i.p. gabapentin (positive control), or vehicle. Animals were re-tested on the rotarod 1, 3, 5 and 24 h following drug administration. In separate experiments, rats received 30, 100, or 300 mg/kg p.o. CBZ, 10, 30, or 100 mg/kg i.p. LTG, 100 mg/kg i.p. gabapentin (positive control) or vehicle, and were tested according to the same schedule.

Acute analgesia

The effect of PPPA on acute analgesia was investigated using the tail flick assay. Rats (n = 9-12/group) were placed on the apparatus (Ugo Basile; Varese, Italy) and an infrared beam was focused onto the tail, 5 cm from the tip. The latency to tail flick was assessed. Cut-off was set at 20 seconds and the intensity was set to 35%. Latency was determined once for each rat at each time point. Baseline latency was determined and approximately 1 h later the rats received a single dose of either 1, 3, or 10 mg/kg PPPA, 10 mg/kg morphine or vehicle. Latencies were determined again 1, 3 and 5 h post drug administration.

Statistical analysis

Data are presented as the mean ± SEM. Untransformed data (thresholds / latencies) were analyzed using a one-way analysis of variance (ANOVA). In instances where a main effect was detected, planned comparisons were made using Fisher's PLSD post hoc analysis. The level of significance was set at $P < 0.05$. Minimal effective dose (MED) and minimal ataxic dose (MAD), represent the lowest tested dose that resulted in a statistically different result as compared to vehicle treated rats at any time point tested.

RESULTS

State-dependent inhibition of rNa$_v$1.2 channels by PPPA

Voltage dependence of inhibition rNa$_v$1.2 currents in HEK-293 cells are half-maximally activated by depolarization from –120 mV to -18.2 ± 0.3 mV (n=13) with a steepness of 5.7 ± 0.3 mV and reach maximum at ~0 mV (Ilyin et al., 2005). With 100 ms depolarizing conditioning pre-pulses, half-maximal inactivation occurs at -53.9 ± 1.7 mV with the slope of 6.4±0.1 mV per e-fold change in membrane potential (n=17). The currents were >95% inactivated at membrane voltages above -20 mV.

Exploratory studies showed that inhibition of recombinant Na^+ currents by PPPA was clearly voltage-dependent. For example, when the holding voltage was set at -120 mV, 1 μM PPPA blocked only 5% of peak current (figure 1, A). But when the holding voltage was -70 mV, inhibition rose to 85% (figure 1, B). At 1 μM, PPPA did not obviously affect the time course of either activation or inactivation of I_{Na} or the voltage-dependence of activation (data not shown). The inhibition was fully reversible upon removal of the drug, though at depolarized voltages the recovery required a longer interval of wash: as an example, the time constant of the wash-out of PPPA, 3 μM was 35 ± 4 s (n=4) and 96 ± 9 s (n=4) at -120 mV and -80 mV, respectively (P < 0.006). The profound voltage-dependence of inhibition is qualitatively consistent with PPPA preferentially binding to Na^+ channels in their inactivated states rather than to the resting states. Thus, the overall affinity of the drug towards the channel at any membrane voltage is a weighted average of the affinity towards resting and inactivated states and should increase with depolarization as the proportion of inactivated channels increases.

Inhibition of resting channels The dissociation constant K_R towards resting state was estimated by measuring the degree of inhibition of the peak I_{Na} elicited by depolarizing pulses from a rather negative membrane voltage, i.e. –120 mV (figure 1, A), assuring nearly zero steady-state

inactivation. At this voltage, block of the peak I_{Na} is weak since the affinity of the drug towards resting channels is low. Assuming 1:1 binding ratio, K_R, calculated / extrapolated from the equation K_R = {Fractional response/(1-Fractional response)}*[antagonist] was 22 $\pm$ 5 μM (n=10) (Table 1).

Retardation of repriming kinetics In the absence of drug, recovery of $rNa_v1.2$ channels from inactivation caused by 1 s long depolarizing pre-pulse from -120 mV to -20 mV was biphasic. About 90% of channels recovered with a time constant of ~5.0 ms and the remaining 10% with a time constant of >500 ms (figure 1, C; also see Ilyin et al., 2005). In 1 μM PPPA, the fast component of recovery was retarded to 53 $\pm$ 5 ms (n=8) (Table 1), while the slower component was essentially unchanged. Retardation of recovery did not depend on PPPA concentration: the repriming constant was 62 $\pm$ 3 ms (n=3) and 60 $\pm$ 4 ms (n=3) for PPPA 0.1 and 1.0 μM, respectively, when measured at -120 mV in one and the same cell (P < 0.2). The lack of concentration-dependence of repriming time constant is easy to understand given that the transition from the state "PPPA bound to inactivated channel" to the state "PPPA bound to resting channel" is a monomolecular reaction (e.g. see the kinetic schema in Ilyin et al., 2005) and thus it should not depend on the drug concentration. This transition is strongly affected by the membrane voltage. Hyperpolarization promotes faster recovery from inactivation both in control and in the presence of drug (data not shown).

Binding kinetics Significant retardation of repriming from inactivation by PPPA provided a way to measure the rate of binding and affinity of the drug to inactivated channels using a double-pulse protocol. The duration of the conditioning pre-pulse, from -120 mV to -20 mV, was increased in increments of 10-40 ms, while the duration of the hyperpolarizing gap was set at 5 ms. The 5 ms gap produced only a negligible contribution of the recovery of non-liganded channels. Thus, the decrease in the amplitude of I_{Na}, when compared to the current in control, was a satisfactory measure of drug-bound (and inhibited) inactivated channels. Subsequent episodes of

stimulation were repeated every 15 s to allow all the recovery processes to occur. Figure 2, A and B show examples of I_{Na} traces obtained from this type of experiment. Under control conditions, the peak I_{Na} showed only a slight trend to drop with the duration of the depolarizing pre-pulse. Whereas in the presence of 0.03 μM PPPA, the current decreased in subsequent stimulation episodes due to progressive binding of the drug to inactivated channels. Binding reached its apparent steady-state at the pre-pulse duration of 480 ms (the 12th stimulation cycle). The drug was potent causing about 50% inhibition at 0.03 μM. The amplitude of the peak I_{Na} was plotted against the duration of the inactivating pre-pulse to give the binding curve. Contamination with non-recovered fast inactivating and slow inactivating channels was corrected by calculating the difference between I_{Na} in control and in the presence of PPPA. The corrected time course of inhibition was well fit by a mono-exponential (figure 2, C). Figure 2, D shows that the microscopic binding rates increase linearly with drug concentration consistent with Langmuir binding theory. This supports the idea that PPPA, and other inhibitors of this class, bind to Na^+ channels in a simple 1:1 mode. From the linear fit, the microscopic rate constant k_+ (the pseudo-first order rate constant) for PPPA binding to the inactivated channels was ~97 μM^{-1} s^{-1} (Table 1). This value indicates that the binding of PPPA to inactivated channels is fast, but is still about an order of magnitude slower than the rate of diffusion-limited reactions.

Affinity for the inactivated state To estimate the apparent dissociation constant (K_I) of PPPA for inactivated $rNa_v1.2$ channels we constructed partial, steady-state concentration-inhibition curves and fit the data with the Hill equation: $1/(1 + ([PPPA]/ K_I)^p)$ where p is the slope (figure 3, A). The K_I was 0.041±0.008 μM (n=5) (Table 1). The slope of the individual fits varied between 0.7 and 1.0.

Use-dependent block In addition to the voltage-dependent inhibition observed with low excitation frequencies (<0.5 Hz) state-dependent blockers can also produce the phenomenon of

use-dependence, where inhibition is enhanced during sustained or higher frequency depolarizations. Mimicking the repetitive discharge seen in hyper-excitable neurons, we assessed the ability of PPPA to "filter" high –frequency electrical activity by measuring use-dependent block of trains of depolarizing voltage pulses of varying frequency. Figure 3, B shows the amplitudes of currents evoked by 10 Hz trains of twenty 5 ms pulses from –70 (the voltage with <10% of channels in inactivated state) to 0 mV in control conditions and in the presence of PPPA, 0.1 and 3 μM. In control, there was a small steady decline in the current amplitude. In the presence of PPPA there was an additional decline in the current due to accumulation of use-dependent block. The use-dependent block became more pronounced with increasing concentration of the drug and frequency of the pulse train (data not shown). A stimulus frequency of 10 Hz was sufficient to clearly show use-dependent block with 0.1 μM PPPA, whereas with 3 μM PPPA the block became very strong.

The results of studies on inhibition of rNa_v1.2 channels in HEK-293 cells by PPPA are summarized in Table 1.

Inhibition of native Na^+ currents in rat DRG neurons

In acute DRG neuron cultures (days 1 to 4 after plating) almost every cell showed a mixture of TTX-R and TTX-S Na^+ currents. As reported previously (e.g. Rush et al., 1998), these currents differed kinetically, TTX-R currents being slower in both activation and inactivation. Superfusion of the chamber with TTX, 200-400 nM was used to isolate the TTX-R components of the currents and voltage-gated Ca^{2+} currents were blocked 0.1 mM $CdCl_2$. The number of cells expressing pure TTX-S currents was relatively small in newly made cultures, but increased with time. By the second week in culture almost 90% cells expressed only TTX-S currents. The potential "contamination" of the current with TTX-R component was checked at the end of experiments by application of 0.2 μM TTX. This concentration was more than sufficient to block

JPET Fast Forward. Published on May 25, 2006 as DOI: 10.1124/jpet.106.104737
This article has not been copyedited and formatted. The final version may differ from this version.

all TTX-S channels ($K_I \leq 20$ nM) but left intact any underlying TTX-R channels / currents ($K_I \geq 50$ μM).

TTX-R currents Of the different TTX-R currents seen in DRG neurons (figure 4, A) we assessed PPPA effects on the component (R1) that activates close to –30 mV, peaks at around 0 mV and shows relatively slow but profound inactivation with V_{half} of –35 mV (complete at 0 mV) (Rush et al., 1998; Lai et al., 2004). There is now compelling evidence to suggest that $Na_v1.8$-containing channels are the major channels underlying this high-threshold TTX-R current (Lai et al., 2004). A double-pulse protocol was again used to measure K_I. In this case, the holding voltage was -90 mV. One second long conditioning pre-pulse to –10 mV elicited Na^+ current that inactivated by the end of the depolarization. Then a 5 ms hyperpolarizing gap (to –90mV) was applied to recover non-liganded channels from the fast inactivation. The subsequent test pulse to 0 mV was used to assay the fraction of the channels available for activation. The protocol was run before and after drug application (figure 4, C - E). Even under control conditions, the size of the current to the second pulse was ~20% of the current to the first pulse. This was due to marked slow inactivation of TTX-R1 channels, which needed a few seconds at polarized potentials for recovery. Nevertheless, the size of the test current was still big enough to assay inhibition caused by PPPA (figure 4, D). Fractional inhibition was collected for various concentrations of the blocker and used to draw the partial concentration-inhibition curve as shown in figure 3. The K_I was 0.046 ± 0.014 μM (n=5) (Table 2).

TTX-sensitive currents. For assaying effects on TTX-S currents, the holding voltage was -120 mV, with a 1 s prepulse to –10 mV (causing complete inactivation), followed by 5 ms hyperpolarizing gap (-120 mV) and a test pulse to 0 mV. The protocol was run before and after drug application. The current traces looked similar to those shown in figure 1. The overall kinetics of the TTX-S current was faster and, in the absence of drug, a 5 ms hyperpolarizing gap was sufficient for >85% channels to recover from inactivation. The fractional responses were

measured at three different concentrations of PPPA to plot partial concentration-inhibition curves. The K_I was 0.011 ± 0.001μM (n=3) (Table 2).

Inhibition of rNa$_v$1.2 channels and native rat DRG neuron currents by CBZ and LTG

For comparison purposes, we characterized inhibition of Na^+ channels by the clinically relevant drugs carbamazepine and lamotrigine.

rNa$_v$1.2 channels Biophysical parameters for CBZ and LTG inhibition of recombinant rNa$_v$1.2 channels are given in Table 1 (Ilyin et al., 2005). In addition, PPPA was compared to the anticonvulsants in its capacity to filter electrical discharge as assessed by inhibition of 20 Hz trains of 40 depolarizing pulses from - 70 mV to 0 mV. When administered at concentrations giving comparable steady-state inhibition, PPPA, 0.1 μM, LTG, 30 μM and CBZ, 50 μM, the drugs inhibited the 40th pulse by 13.5±3.2 % (n=4), 15.5±2.0 % (n=3) and 17±1.6% (n=3), respectively. However, steady-state inhibition was achieved appreciably faster for PPPA (τ=4.5±0.6 s, n=4) than for CBZ (τ=8.7±3.2 s, n=3) and LTG (τ=25±10.6 s, n=3). The difference was not significant for comparison of PPPA and CBZ (P<0.08), but was significant when compared with LTG (P<0.02).

Neuronal recordings Protocols for isolated DRG neurons recordings using CBZ and LTG were identical to those described for PPPA. K_I values for CBZ and LTG inhibition of TTX-R and TTX-S Na^+ currents are given in Table 2. As seen with the recombinant channels, PPPA was significantly more potent than classical anticonvulsants (P<0.001).

PPPA does not block voltage-gated N-type Ca^{2+} channels in human neuroblastoma IMR-32 cells

In the concentration range tested, PPPA showed no inhibition of Ca^{2+} signal in FLIPR^{96} (IC_{50}> 20 μM (n=4), data not shown). In the same experimental series, ω-ctx MVIIA, a selective blocker

JPET Fast Forward. Published on May 25, 2006 as DOI: 10.1124/jpet.106.104737
This article has not been copyedited and formatted. The final version may differ from this version.

of N-type Ca^{2+} channels, inhibited the fluorescent signal with an IC_{50} = 46.6 $\pm$ 10.8 nM (n=4) (data not shown).

PPPA reduces hyperalgesia following nerve injury

Partial ligation of the sciatic nerve resulted in mechanical hyperalgesia present 21 days after surgery (Table 3; figure 5, A). Administration of PPPA (3-30 mg/kg, p.o.) produced a dose-dependent inhibition of mechanical hyperalgesia 1 ($F_{(5,40)}$=10.39, P < 0.0001), 3 ($F_{(5,40)}$=5.56, P = 0.0006), and 5 hours ($F_{(5,40)}$=7.81, P < 0.0001) after administration. PPPA (30 mg/kg) significantly increased PWTs 1, 3, and 5 hours after administration, whereas administration of 3 or 10 mg/kg PPPA produced a significant effect only at the 3 hour time point. The antihyperalgesic effects of PPPA were no longer evident 24 hours after dosing. The efficacy of 30 mg/kg PPPA was similar to, and the duration of action was greater than that of the positive control, gabapentin (100 mg/kg, i.p.). The antihyperalgesic effects of PPPA were limited to the injured paw; there was no effect of PPPA on PWTs in the contralateral paw (data not shown).

PPPA reduces hyperalgesia associated with inflammation

Injection of 50 μL of 50% FCA resulted in mechanical hyperalgesia 24 hours after injection as indicated by decreased PWTs (Table 3; figure 5, B). PPPA administration (1-10 mg/kg, p.o.) produced a significant reduction in FCA-induced mechanical hyperalgesia 1 ($F_{(5,53)}$ = 7.933, P = 0.0001), 3 ($F_{(5,53)}$ = 6.389, P = 0.0001), and 5 hours ($F_{(5,53)}$ = 6.297, P = 0.0001) after dosing. Administration of 30 mg/kg PPPA produced significant antihyperalgesia 1, 3, and 5 hours after dosing, while administration of 3 mg/kg PPPA resulted in a significant reduction in hyperalgesia only at the 3 hour time point. There were no significant effects of PPPA administration on FCA-induced mechanical hyperalgesia 24 hours after dosing. The efficacy and the duration of action of PPPA against FCA-induced mechanical hyperalgesia were similar to, or greater than, the positive control celecoxib (30 mg/kg, p.o.).

JPET Fast Forward. Published on May 25, 2006 as DOI: 10.1124/jpet.106.104737
This article has not been copyedited and formatted. The final version may differ from this version.

PPPA reduces mechanical hyperalgesia induced by paw incision

Incision of the plantar surface of the hind paw resulted in the development of mechanical hyperalgesia 24 hours after surgery (Table 3). Administration of PPPA (0.3-30 mg/kg, p.o.) resulted in a dose-dependent reduction in mechanical hyperalgesia 1 ($F_{(7,112)}$ = 25.416, P < 0.0001), 3 ($F_{(7,112)}$ = 20.051, P < 0.0001), and 5 hours ($F_{(7,112)}$ = 21.495, P < 0.0001) after dosing (figure 5, C). Administration of 30 mg/kg PPPA significantly reduced incision-induced hyperalgesia 1 and 3 hours after dosing, and administration of 3 or 10 mg/kg PPPA resulted in a significant reduction in mechanical hyperalgesia at the 3 hour time point only. There was no effect of PPPA administration on mechanical hyperalgesia 24 hours after dosing. The maximum reversal of mechanical hyperalgesia by PPPA was comparable to that produced by the positive control indomethacin (30 mg/kg p.o.).

PPPA has no effect on acute nociception

Administration of PPPA (1-10 mg/kg, p.o.) had no effect on acute nociception as measured by the tail flick assay (Table 3). Tail flick latencies were measured 1, 3, and 5 hours after drug administration. The positive control, morphine (10 mg/kg, s.c.), produced significant antinociception 1, 3, and 5 hours after drug administration (P <0.0001, Fisher's PLSD test at each time point).

PPPA has no effect on motor performance

Administration of PPPA (3-30 mg/kg, p.o.) did not induce ataxia nor did it have other effects on motor performance as measured by the accelerating rotarod assay (Table 4). Latencies to fall-off of the rotarod apparatus were measured 1, 3, 5 and 24 hours after drug administration. While there was no effect of PPPA on motor performance, the positive control, gabapentin (100 mg/kg, i.p.) resulted in significant motor deficits 1, 3, and 5 hours after administration.

Efficacy and side effect profiles of carbamazepine and lamotrigine

As reported previously (Hunter et al., 1997), CBZ and LTG each produced significant reversal of nerve injury-induced mechanical hyperalgesia as well as significant motor impairment as measured by the rotarod assay. Administration of CBZ (1-100 mg/kg, p.o.) three weeks after partial ligation of the sciatic nerve resulted in a significant reversal of mechanical hyperalgesia with a minimum effective dose (MED) of 100 mg/kg, 1 and 3 hours after administration. When the effect of CBZ on motor performance was measured, the minimal ataxic dose (MAD) was 30 mg/kg 1 hour after administration, rising to 300 mg/kg 3 hours after drug administration. Therefore the therapeutic index (TI) for CBZ was 0.3 at 1 hour and 3 at 3 hours after drug administration (Table 4).

The efficacy and side effect profiling of LTG was similar to that of CBZ. Administration of LTG (3-100 mg/kg, i.p.) produced a dose-dependent reversal of nerve injury-induced mechanical hyperalgesia 1, 3, and 5 hours after administration. At each of these time points, the MED of LTG was 30 mg/kg. LTG also induced profound motor deficits after administration, with a MAD of 30 mg/kg 1 and 5 hours after administration, and 10 mg/kg 3 hours after drug administration. As such, the TI for LTG was 1 at 1, 3 and 5 hours after drug administration (Table 4).

DISCUSSION

PPPA is a potent, state-dependent blocker of voltage-gated Na^+ channels. Assayed on recombinant $rNa_V1.2$ channels and native Na^+ currents in rat DRG neurons PPPA has ~1000 times higher potency and >2000-fold faster onset kinetics than the clinical comparators CBZ and LTG. Moreover, PPPA has ~10-20-fold higher levels of selectivity for inactivated channels versus resting-state channels (i.e. state-dependence) than CBZ and LTG. PPPA was inactive against N-type Ca^{2+} channels in IMR-32 cells and across a standard panel of CNS targets (NovaScreen, General Side Effects Profile I). In vivo studies show that PPPA is potent and efficacious in reversing mechanical hyperalgesia in rat models of neuropathic, post surgical and inflammatory pain. PPPA has no effect on paw withdrawal thresholds in the contralateral paw, or in models of acute thermal nociception, indicating that efficacy is not due to a local anesthetic-like nerve block. Importantly, PPPA has a TI >10 versus ataxia. PPPA, CBZ and LTG all have limited (<10-fold) levels of subtype-selectivity for different recombinant Na^+ channel subtypes and native Na^+ currents (V.I. Ilyin, unpublished data). Thus it appears that differences in the biophysics of Na^+ inhibition confer PPPA with an improved efficacy to side effects profile compared to anticonvulsants like CBZ and LTG.

Studies investigating CBZ and LTG in rat neuropathic pain models are limited and direct comparisons with the current work are difficult due to differences in rat strain, model, routes of administration and behavioral measurement (e.g. Hunter et al., 1997; Erichsen et al., 2003; Decosterd et al., 2004; Lindia et al., 2005). In most cases, however, doses associated with efficacy in neuropathic pain models are in the same range that would have produced ataxic / sedative effects in our accelerating rotarod assay. Thus for CBZ and LTG it is difficult to distinguish ‘efficacy’ from side effects. This lack of TI in rats appears to translate directly to a poor therapeutic index for treating neuropathic pain in humans (Mao and Chen, 2000; Jensen, 2002; Petersen et al., 2003). In contrast, PPPA has a TI >10, suggesting a meaningful

separation between doses that are efficacious in reversing mechanical hyperalgesia and those producing ataxia. To confirm this, exploratory pharmacokinetic studies in rats were conducted and showed that, in the range 1-30 mg/kg p.o., PPPA has dose-proportional increases in C_{max} and AUC, with a half-life of ~6 h, and oral bioavailability of ~100% (Y. Rotstheyn and P. Bullock, unpublished results). This indicates PPPA has a TI that is >10 both in terms of dose and, more importantly, in terms of drug exposure (C_{max}). Na^+ channel blockers are widely used clinically to treat neuropathic pain (e.g. Mao and Chen, 2000; Jensen, 2002; Petersen et al., 2003). In contrast, their effectiveness for treating other types of human pain, for example pain associated with osteoarthritis, visceral pain arising from gastrointestinal disorders and post surgical pain (beyond their use of local anesthetics) is minimal or unreported. To further explore the therapeutic potential of PPPA as an analgesic it will be worthwhile to test the compound in more sophisticated animal models of osteoarthritis and in models of visceral pain (Laird et al., 2001; Blackburn-Munro et al., 2002; Su et al., 2002).

The results of our study suggest that the biophysical parameters of Na^+ channels inhibition contribute to an improved TI for PPPA as compared to CBZ and LTG, however, the exact mechanism(s) remains unclear. Pathological nerve hyperexcitability is characterized by sustained depolarizations with superimposed high-frequency bursts of action potentials. Under these conditions, Na^+ channels accumulate in inactivated states and their availability for repetitive excitation is lowered. An additional reduction in the channel availability by drug-induced use-dependent block is thought to lead to selective attenuation of spike bursts in the depolarized neurons. PPPA exerts highly state-dependent block of Na^+ channels. For $rNa_v1.2$, PPPA discriminates inactivated versus resting channels with a factor of K_R/K_I > 500-fold (Table 1). Such a high level of state-dependence minimizes the risk of interfering pharmacologically with signaling in non-pathological neuronal circuits. Levels of state-dependence for CBZ (~30-fold) and LTG (~60-fold) are substantially lower.

JPET Fast Forward. Published on May 25, 2006 as DOI: 10.1124/jpet.106.104737
This article has not been copyedited and formatted. The final version may differ from this version.

Another biophysical parameter that could contribute to PPPA's improved TI is onset-binding kinetics. The on-rate of binding of PPPA to inactivated channels is comparatively fast. At equimolar concentrations, PPPA binds to the inactivated $Na_V1.2$ channels >2,000 times faster than CBZ and LTG. If the drugs are available at their respective K_I values, a more reasonable assumption for the situation in vivo at efficacious doses, room temperature microscopic rates of binding (the product of K_I and k_+) are ~4 s^{-1}, ~1.8 s^{-1} and 0.7 s^{-1} for PPPA, CBZ and LTG, respectively. This means PPPA exerts a 2- to 6-fold faster, and more pronounced, block of hyperexcitability episodes of comparable durations, which may be important in pain states where hyperexcitability hinges on the short-lived inactivated states (Rush et al., 1998; Waxman et al., 2000).

Retardation of recovery from inactivation is another feature of state-dependent block of voltage-gated Na^+ channels and underlies use (or frequency)-dependent inhibition (Ilyin et al., 2005). Interestingly, though highly potent, PPPA shows only moderate levels of retardation, i.e. ~70% of channels recovered from inactivation with τ_{repr}~53 ms, which are comparable to LTG and CBZ (Table 1). In this respect, PPPA and the two anticonvulsants are very different from anesthetics such as bupivacaine, which retards repriming for many seconds (V. I. Ilyin, unpublished observations). Modest effects on retardation may be important to minimize the impact on non-pathological neuronal activity, particularly in the CNS.

As compared to PPPA, the prototype compound V102862 (Ilyin et al., 2005) was ~ 20-fold and ~ 6-fold less potent on native TTX-S and TTX-R currents in rat DRG neurons. On the recombinant $rNa_v1.2$ channels, V102862 was ~10-less potent than PPPA in binding to inactivated channels and had a lower state-dependency ratio $K_r/K_i \simeq 70$. At equal concentrations V102862 was 50-fold slower in binding to inactivated channels; at the same time it caused more significant retardation of repriming from inactivation ($\tau_{repr} \simeq 700$ ms at V_h=-120 mV as compared

to ~50 ms for PPPA). From mechanistic point of view, higher potency combined with higher rate of binding to inactivated channels may provide PPPA an advantage in exerting higher levels of inhibition of sodium channels within shorter intervals of hyperexcitability. The experiments with frequency pulse trains similar to that shown in fig. 3, B support this hypothesis: at 3 μM PPPA caused steady-state inhibition of ~60% at the 2nd pulse in the train as compared 34% inhibition seen at the 20th pulse for V102862 (V.I. Ilyin, unpublished data). This feature may play especially important role for effective blocking of rapidly repriming TTX-R channels in DRG neurons (Rush et al., 1998) during short episodes of hyperexcitability.

There is now little question, at least in rat pain models, that Na^+ channel regulation contributes to hyperexcitability of primary afferent neurons after nerve injury and inflammation (for reviews see Waxman et al., 2000; Lai et al., 2004; Priestley, 2004). However, recent data also calls into question whether selective inhibition of a single subtype of Na^+ channel, e.g. $Na_V1.8$ or $Na_V1.7$, will be sufficient to produce robust analgesic effects across diverse pain states (Lindia et al., 2005; Nassar et al., 2005). The improved TI of PPPA, in the absence of clear subtype-selectivity, suggests that researchers reporting on novel subtype-selective blockers (e.g. Silos-Santiago et al., 2005), should be cautious in ascribing improvements in TI to subtype-selectivity as opposed to more optimal biophysical parameters (Brochu et al., 2006).

Whether PPPA acts both centrally and peripherally and which is more important in the various pain settings is unknown. Separate experiments showed that PPPA is active in a rat model of maximum electroshock-induced seizures over the same dose range (ED_{50} = 2.5 mg/kg p.o.) and time course that produced efficacy in the pain models (K. Vanover and R. Carter, unpublished results). This clearly implies that PPPA has access to the CNS. Drug levels of CBZ and LTG in the CSF at clinical therapeutic doses are ~13 μM and ~20 μM, respectively (e.g. Kuo and Lu, 1997). If approximately the same free drug levels are found in the periphery, the

anticonvulsants reach sufficient levels to block central and peripheral TTX-S currents but will have little effect on TTX-R currents in primary afferents, where the K_I's are >100 μM (Table 2). PPPA is ~2000 times more potent at blocking TTX-R currents. Therefore PPPA blockade of TTX-S currents, centrally and peripherally, ***combined*** with blockade of peripheral TTX-R currents, may be contributing to the improved potency, efficacy and TI.

In conclusion, alterations in the excitability of injured neurons underlie spontaneous pain, allodynia and hyperalgesia. Numerous different Na^+ channel subtypes appear to play roles in establishing and maintaining ectopic discharge in primary afferent neurons and hyperexcitability in the periphery and CNS. PPPA's broad activity in pain models and improved TI suggest that potent, state-dependent, broad spectrum Na^+ channel blockers will have utility for treating pain in humans.

JPET Fast Forward. Published on May 25, 2006 as DOI: 10.1124/jpet.106.104737
This article has not been copyedited and formatted. The final version may differ from this version.

ACKNOWLEDGEMENTS

The authors would like to acknowledge the work of Dr. Dianne D. Hodges in establishing rNaIIA-B2 ($rNa_v1.2$)–HEK-293 cell line and Daniela Leumer, Silvia Robilos and Michael Suruki for their technical support and Dr. Kenneth Valenzano for critical reading of the manuscript.

REFERENCES

Akopian AN, Souslova V, England S, Okuse K, Ogata N, Ure J, Smith A, Kerr BJ, McMahon SB, Boyce S, Hill R, Stanfa L, Dickenson AH and Wood JN (1999) The tetrodotoxin-resistant sodium channel SNS has a specialized function in pain pathways. *Nat Neurosci* **2**:541-548.

Blackburn-Munro G, Ibsen N and Erichsen HK (2002) A comparison of the anti-nociceptive effects of voltage-activated Na^+ channel blockers in the formalin test. *Eur J Pharmacol* **445**:231-238.

Brennan TJ, Vandermeulen EP and Gebhart GF (1996) Characterization of a rat model of incisional pain. *Pain* **64**:493-501.

Brochu RM, Dick IE, Tarpley JW, McGovan E, Gunner D, Herrington J, Shao PP, Ok D, Li C, Parsons WH, Stump GL, Regan CP, Lynch JJ, Lyons KA, McManus OB, Clark S, Ali Z, Kaczorowski GJ, Martin WJ and Priest BT (2006) Block of peripheral nerve sodium channels selectively inhibits features of neuropathic pain in rats. *Mol Pharmacol* **69**:823-832.

Catterall WA (2000) From ion currents to molecular mechanisms: the structure and function of voltage-gated sodium channels. *Neuron* **26**:13-25.

Chahine M, Ziane R, Vijayaragavan K and Okamura Y (2005) Regulation of Na_v channels in sensory neurons. *Trens Pharmacol Sci* **26**:496-502.

Coggeshall RE, Tate S and Carlton SM (2004) Differential expression of tetrodotoxon-resistant sodium channels $Na_v1.8$ and $Na_v1.9$ in normal and inflamed rats. *Neurosci Lett* **355**:45-48.

Coward, K, Plumpton C, Facer P, Birch R, Carlstedt T, Tate S, Bountra C and Anand P (2000) Immunolocalization of SNS/PN3 and NaN/SNS2 sodium channels in human pain states. *Pain* **85**:41-50.

Craner MJ, Klein JP, Renganathan M, Black JA and Waxman SG (2002) Changes of sodium channel expression in experimental painful diabetic neuropathy. *Ann Neurol* **52**:786-792.

Decosterd I, Allchorne A and Woolf CJ (2004) Differential analgesic sensitivity of two distinct neuropathic pain models. *Anesth Analg* **99**:456-463.

De Vry J, Kuhl E, Franken-Kunkel P and Eckel G (2004) Pharmacological characterization of the chronic constriction injury model of neuropathic pain. *Eur J Pharmacol* **491**:137-148.

Dimmock JR, Puthucode RN, Smith JM, Hetherington M, Quail JW, Pugazhenthi U, Lechler T and Stables JP (1996) (Aryloxy)aryl semicarbazones and related compounds: a novel class of anticonvulsant agents possessing high activity in the maximal electroshock screen. *J Med Chem* **39**: 3984-3998.

Erichsen HK, Hao J-X, Xu X-J and Blackburn-Munro G (2003) A comparison of the antinociceptive effects of voltage-activated Na^+ channel blockers in two rat models of neuropathic pain. *Eur J Pharmacol* **458**:275-282.

Gold MS, Weinreich D, Kim KS, Wang R, Treanor J, Porreca F and Lai J (2003) Redistribution of $Na_v1.8$ in uninjured axons enable neuropathic pain. *J Neurosci* **23**:158-166.

Goldin AL (2001) Resurgence of sodium channel research. *Annu Rev Physiol* **63**:871-894.

Hains BC, Saab CY, Klein JP, Craner MJ and Waxman SG (2004) Altered sodium channel expression in second-order spin sensory neurons contributes to pain after peripheral nerve injury. *J Neurosci* **19**:4832-4839.

Hong S, Morrow TJ, Paulson PE, Isom LL and Wiley JW (2004) Early painful diabetic neuropathy is associated with differential changes in tetrodotoxin-sensitive and -resistant sodium channels in dorsal root ganglion neurons in the rat. *J Biol Chem* **279**:29341-29350.

Hunter JC, Gogas KR, Hedley LR, Jacobson LO, Kassotakis L, Thompson J and Fontana DJ (1997) The effect of novel anti-epileptic drugs in rat experimental models of acute and chronic pain. *Eur J Pharmacol* **18**:153-160.

Ilyin VI, Hodges DD, Whittemore ER, Carter RB, Cai S-X and Woodward RM (2005) V102862 (Co 102862): a potent, broad-spectrum, state-dependent blocker of mammalian voltage-gated sodium channels. *Br J Pharmacol* **144**:801-12.

Isom LL (2001) Sodium channel beta subunits: anything but auxillary. *Neuroscientist* **7**:42-54.

Jensen TS (2002) Anticonvulsants in neuropathic pain: rationale and clinical evidence. *Eur J Pain* **6**:61-68.

Kiguchi S, Imamura T, Ichikawa K and Kojima M (2004) Oxcarbazepine antinociception in animals with inflammatory pain or painful diabetic neuropathy. *Clin Exp Pharmacol Physiol* **31**:57-64.

Kuo C-C and Lu L (1997) Characterization of lamotrigine inhibition of Na^+ channels in rat hippocampal neurons. *Br J Pharmacol* **121**:1231-1238.

Lai J, Gold MS, Kim CS, Bain D, Ossipov MH, Hunter JC and Porreca F (2002) Inhibition of neuropathic pain by decreased expression of the tetrodotoxin-resistant sodium channel, $Na_v1.8$. *Pain* **95**:143-152.

Lai J, Porreca F, Hunter JC and Gold MS (2004) Voltage-gated sodium channels and hyperalgesia. *Annu Rev Pharmacol Toxicol* **44**:371-97.

Laird JMA, Carter AJ, Grauert M and Cervero F (2001) Analgesic activity of a novel use-dependent sodium channel blocker, crobenetine, in mono-arthritic rats. *Br J Pharmacol* **134**:1742-1748.

Laird JMA, Souslova V, Wood JN and Cervero F (2002) Deficits in visceral pain and referred hyperalgesia in $Na_v1.8$ (SNS/PN3)-null mice. *J Neurosci* **22**:8352-8356.

Lindia JA, Kohler MG, Martin WJ and Abbadie C (2005) Relationship between sodium channel $Na_V1.3$ expression and neuropathic pain behavior in rats. *Pain* **117**:145-153.

Mao J and Chen LL (2000) Systemic lidocaine for neuropathic pain relief. *Pain* **87**:7-17.

Nassar MA, Sterling LC, Forlani G, Baker MD, Matthews EA, Dickenson AH and Wood JN (2004) Nociceptor-specific gene deletion reveals a major role for $Na_v1.7$ (PN1) in acute and inflammatory pain. *Proc Natl Acad Sci USA* **101**:12706-12711.

Nassar MA, Levato A, Stirling LC and Wood JN (2005) Neuropathic pain develops normally in mice lacking both Nav1.7 and Nav1.8. *Mol Pain* **1**:24-32.

Petersen KL, Maloney A, Hoke F, Dahl JB and Rowbotham MC (2003) A randomized study of the effect of oral lamotrigine and hydromorphone on pain and hyperalgesia following heat/capsaicin sensitization. *J Pain* **4**:400-406.

Priestley T (2004) Voltage-gated sodium channels and pain. *Curr Drug Targets – CNS Neurol Dis* **3**:441-456.

Rush AM, Brau ME, Elliott AA and Elliott JR (1998) Electrophysiological properties of sodium current subtypes in small cells from adult rat dorsal root ganglia. *J Physiol (Lond)* **511**:771-789.

Scheuer T, Auld VJ, Boyd S, Offord J, Dunn R and Catterall WA (1990) Functional properties of rat brain sodium channels expressed in a somatic cell line. *Science (Wash DC)* **247**:854-858.

Seltzer Z, Dubner R and Shir Y (1990) A novel behavioral model of neuropathic pain disorder produced in rats by partial sciatic nerve injury. *Pain* **43**:450-456.

Su X, Joshi SK, Kardos S and Gebhart GF (2002) Sodium channel blocking actions of the kappa-opioid receptor agonist U50,488 contribute to its visceral antinociceptive effects. *J Neurophysiol.* **87**:1271-1279.

Takahashi N, Kikuchi S, Dai Y, Kobayashi K, Fukuoka T and Noguchi K (2003) Expression of auxillary β subunits of sodium channels in primary afferent neurons and the effect of nerve injury. *Neuroscience* **121**:441-450.

Waxman SG, Cummins TR, Dib-Hajj SD and Black JA (2000) Voltage-gated sodium channels and the molecular pathogenesis of pain: a review. *J Rehabil Res Dev* **37**:517-528.

FOOTNOTES

Benjamin ER, Chen Z, Sha D, Tafesse L, Victory SF, Whitehead JWF and Zhou X (2006) Piperidinyl compounds and the use thereof. Patent No. WO 2006/040181 A2 (Apr. 20, 2006).

Hogenkamp DJ, Nguyen P and Shao B (2005) Aryl substituted pyrimidines. Patent No. US 6,867,210 B2 (Mar. 15, 2005).

Silos-Santiago I, Nguyen T, Bian D, Wilson D, Fanning D, Termin A, Huang C, Urrutia A, Negulescu P and Gonzalez J (2005) Analgesic activity of a selective Na_v channel blocker in models of nociceptive and neuropathic pain. *11th World Congress on Pain (Sydney)* 1173-P43.

Mail reprint requests to: Victor I. Ilyin, Discovery Research, Purdue Pharma LP, 6 Cedar Brook Drive, Cranbury, NJ 08512.

Present address: Discovery Research, Purdue Pharma LP, 6 Cedar Brook Drive, Cranbury, NJ 08512 (V.I.I. and S.O.); Algos Therapeutics, 1246 University Ave W, Suite 205, St. Paul, MN 55104 (J.D.P. and S.G.); Wyeth Research, CN 8000, Princeton, NJ 08543 (G.T.W. and J.E.H.); Merck and Company, Sumneytown Pike, West Point, PA 19486 (M.S.P.); Schering Plough Research Institute, 2015 Galloping Hill Road, Kenilworth, NJ 07033 (L.M.); 37 York Dr, Apt 3B, Edison, NJ 08817 (P.I.T.); Novartis Pharmaceutical Corporation, One Health Plaza, East Hanover, NJ 07936 (R.B.C.); Allergan, Inc., 2525 Dupont Drive, Irvine, CA 92612 (P.N.); Department of Pharmacology, University of California, Irvine, CA 92697 (D.J.H.); Amicus Therapeutics, 6 Cedar Brook Drive, Cranbury, NJ 08512 (E.B.); Adolor Corporation, 700 Pennsylvania Drive, Exton, PA 19341 (R.M.W.).

LEGENDS FOR FIGURES

Figure 1. Voltage-dependent block of I_{Na} and retardation of recovery from inactivation in rNa$_v$1.2/HEK-293 cells. The currents shown in this and other figures were measured after $\geq$1 min in control or drug-containing solutions, i.e. under steady-state drug binding conditions. I_{Na} were elicited by pulsing to 0 mV (maximal I_{Na}), either from holding potentials of -120 mV (A) or -70 mV (B), first under control conditions and then in the presence of 1 μM PPPA (lower and upper traces in each pair, respectively). Dashed line corresponds to zero current level. (C) Retardation of recovery from inactivation. The rate of recovery from inactivation was assessed using a double-pulse protocol where the depolarizing pre-pulse was followed by a step back to the initial negative holding voltage for varying durations (recovery gap) and then by a test pulse to examine the extent of channel recovery from inactivation (repriming). The holding (and gap) voltage was set at –120 mV to remove residual steady-state inactivation, the conditioning pre-pulse was set to –20 mV, to drive all channels into inactivated states, and the test pulse voltage was 0 mV. Duration of the conditioning pre-pulse was chosen to be sufficiently long (1 s) to permit a steady-state level of binding of the drug to inactivated channels. Hyperpolarizing gap was varied in Δt = 10 ms increments. As presented in the figure, the recovery was measured first in control, then in the presence 1 μM PPPA in three different HEK-293 cells and normalized to the size of current taken without the depolarizing pre-pulse. The double-exponential fit (solid line) was done for the averaged control data set: fast component has τ_1 ~5 ms; slow component has τ_2 >500 ms. In the presence of 1 μM PPPA, the averaged time course of recovery followed a single exponential with τ ~61 ms in this experimental series. *Insert*: the chemical structure of PPPA.

Figure 2. The binding rate of PPPA to inactivated rNa$_v$1.2 channels. (A) Control: from a holding voltage of –120 mV the cell was pulsed in duration increments of 40 ms to –20 mV

every 15 s. Gap voltage (-120 mV, 5 ms) was applied after the depolarizing pre-pulse to recover inactivated and unliganded channels. The 10 ms test pulse to 0 mV gave a measure of channels available for activation. Thirteen successive traces (episodes) were superimposed; downward deflections represent inward Na currents evoked by the test pulses in successive episodes. In control, currents show a small reduction in amplitude with increasing duration of conditioning pre-pulse. (B) Same protocol in the presence of 0.03 μM PPPA. Progressive drop in the size of current over time reflects the increase in the proportion of Na^+ channels bound and inhibited by PPPA. (C) Peak current amplitudes from (A) and (B) were plotted against duration of inactivating pre-pulse to get the binding curves. The time-course of current decay in control (filled circles) was subtracted from the time-course of the decay in the presence of the drug (open circles). The resulting curve (crossed circles) tracks the binding of PPPA to inactivated channels. All three curves were fitted by single exponentials. Two parameters were determined for the binding curve at each particular drug concentration: the time constant, τ, of binding to inactivated channels and fractional response FR in steady-state. The latter was measured as a ratio of peak currents in control and in the presence of the drug. (D) Similar analysis was done for various PPPA concentrations, 0.03, 0.1, 0.3 and 1.0 μM. The microscopic binding rates for PPPA (the inverses of the time constants as measured in (C)) taken from 6 cells and plotted against concentration of the drug. The line is linear regression fit to mean values. The slope is ~97 $\mu M^{-1}s^{-1}$ and numerically equal to the pseudo-first order constant k_+ of PPPA binding to inactivated channels.

Figure 3. (A). A set of semilogarithmic concentration-inhibition curves for inhibition of $rNa_v1.2$ channels by PPPA taken for conditioning (inactivating) pre-pulses to –20 mV in five different cells. Fractional responses were measured in steady-state as illustrated in figure 2, A and B. The curves are the best sigmoidal fits according to the equation $1/(1 + ([PPPA]/K_I)^p)$. (B).

Frequency-dependence (use-dependence) of inhibition of 10 Hz trains of maximal $rNa_v1.2$ currents measured from a holding voltage of –70 mV with 5 ms depolarizing pulses to 0 mV. The peak currents in each train were normalized to the size of the first current in a series and plotted against the pulse number (20 pulses in total). The curves are mono-exponential fits. The size of the current to the 20th depolarizing pulse is: 0.94, 0.69 and 0.40 for control and 0.1 and 3 μM PPPA, respectively.

Figure 4. Traces and I-V curve for TTX-R current, V_h = -90mV. A. Current traces at different depolarizing pulses. Little inactivation is seen with low-threshold, type R2 (Rush et al., 1998) TTX-R current (up to –20 mV). High levels of inactivation are seen for type R1 current measured at 0 mV. B. I-V-curve for the inward current has two distinct peaks at approximately –20 mV and 0 mV. Current reverses at about +55 mV, close to the Nernstian potential for Na^+ ions. (C-E) Measuring fractional response (FR) for inhibition of R1 type TTX-R current in a rat DRG neuron by PPPA. (C) TTX-R current in response to double pulse protocol in control. One second long depolarizing pre-pulse to 0 mV was followed up by the 10 ms hyperpolarizing step back to -90 mV and then by a 10 ms long test pulse to 0 mV. (D) Current in the presence of PPPA, 0.03μM. Calibration bars are the same for (C) and (D). (E) The current traces (from C and D) in response to a second, testing voltage pulse shown at a higher gain and speed. The ratio of peak amplitudes was used as the FR to plot inhibition-concentration curves.

Figure 5. Reversal of mechanical hyperalgesia by PPPA in a rat partial spinal nerve ligation model (A), in a rat FCA model of chronic inflammatory pain (B) and in a rat model of incisional pain (C). Hind paw withdrawal thresholds (PWT) to a noxious mechanical stimulus were determined using a model 7200 analgesymeter (Ugo Basile; Varese, Italy). Cut-off was set at 250 g and the endpoint was taken as complete paw withdrawal. PWT was determined once for

each rat at each time point. Baseline PWTs were taken and either the sciatic nerve was exposed and one third to one half ligated or 50 μL of a 50% FCA solution in saline was injected into the paw or a 1 cm longitudinal incision was made through skin and fascia of the plantar aspect of the paw. Twenty-four hours (FCA and incision) or 21 days (PSN) later, pre-drug PWTs were measured and the rats (n = 9-20/group) received a single dose of PPPA and PWT was again determined 1, 3, 5 and 24 h post drug administration. X axis: base, baseline; pre, pre-drug reading.

JPET Fast Forward. Published on May 25, 2006 as DOI: 10.1124/jpet.106.104737
This article has not been copyedited and formatted. The final version may differ from this version.

TABLES

Table 1. Summary of effects of PPPA, LTG and CBZ on rNa$_v$1.2 channels in HEK-293 cells

Compound	K_R, μM	K_I, μM	k_+, $\mu M^{-1}s^{-1}$	τ_{rep}, ms
PPPA	22±5 (10)	0.041±0.008 (5)	~97 (6)	53±5 (8)
LTG	1800±250 (5)	29±3 (3)	~0.024 (4)	64±3 (3)
CBZ	1300±100 (5)	46±5 (5)	~0.045 (4)	20±1 (3)

Table 2. Summary of effects of PPPA, LTG and CBZ on native TTX-S and TTX-R currents in rat DRG neurons

Compound	TTX-S currents: K_I, μM	TTX-R currents: K_I, μM
PPPA	0.011±0.001(3)	0.046±0.014 (5)
LTG	38.4±4.8 (5)	103±13 (9)
CBZ	28.0±4.7 (3)	111±23 (4)

JPET Fast Forward. Published on May 25, 2006 as DOI: 10.1124/jpet.106.104737
This article has not been copyedited and formatted. The final version may differ from this version.

Table 3. Summary of the in-vivo effects of PPPA*

Plantar incision

		Paw Withdrawal Threshold (grams)					
Treatment	**N**	**Pre-surgery**	**Pre-Drug**	**1 hr**	**3 hrs**	**5 hrs**	**24 hrs**
Naïve/Vehicle	20	181.50 (6.6)	178.00 (10.1)	191.50 (8.1)	187.25 (8.8)	184.25 (7.0)	181.50 (6.3)
INC/Vehicle	20	179.75 (5.4)	67.00 (10.0)	79.00 (7.7)	80.25 (7.3)	80.25 (7.3)	78.75 (5.8)
INC/PPPA 0.3 mg/kg	10	179.0 (6.5)	67.0 (10.0)	73.5 (10.8)	81.5 (11.9)	72.0 (9.6)	72.0 (10.4)
INC/PPPA 1 mg/kg	10	192.5 (9.4)	68.00 (9.7)	87.00 (10.5)	104.00 (8.5)	85.5 (10.6)	72.5 (11.1)
INC/PPPA 3 mg/kg	20	179.75 (7.3)	66.50 (5.0)	98.75 (4.2)	**122.75 (6.0)**	91.75 (7.5)	72.5 (5.7)
INC/PPPA 10 mg/kg	11	171.82 (4.9)	115.00 (4.4)	**106.36 (9.9)**	**112.73 (8.9)**	85.00 (11.0)	59.09 (7.2)
INC/PPPA 30 mg/kg	9	170.56 (5.3)	36.67 (7.1)	**115.56 (11.6)**	**120.56 (11.0)**	98.89 (18.3)	60.56 (11.4)
INC/Indometh. 30 mg/kg	20	179.75 (7.3)	66.5 (5.0)	**98.75 (4.2)**	**122.75 (6.0)**	91.75 (7.5)	72.5 (5.7)

Rotarod Assay

		Latency to Fall (seconds)				
Treatment	**N**	**Baseline**	**1 hr**	**3 hrs**	**5 hrs**	**24 hrs**
Vehicle	10	185.82 (10.9)	277.61 (13.2)	127.02 (15.5)	201.99 (23.1)	215.90 (16.1)
PPPA 3 mg/kg	10	185.00 (10.7)	270.00 (11.7)	252.46 (20.0)	192.74 (16.2)	201.59 (20.3)
PPPA 10 mg/kg	10	185.30 (9.2)	293.41 (6.2)	259.45 (17.5)	238.67 (17.8)	238.45 (18.2)
PPPA 30 mg/kg	10	186.16 (9.78)	279.35 (12.8)	247.83 (23.7)	198.45 (13.4)	208.95 (16.1)
Gabapentin 100 mg/kg	10	184.99 (10.1)	**155.49 (23.8)**	**146.79 (17.9)**	**138.66 (20.5)**	213.17 (16.9)

Tail Flick Assay

		Tail Flick Latency (seconds)			
Treatment	**N**	**Baseline**	**1 hr**	**3 hrs**	**5 hrs**
Vehicle	10	5.79 (0.6)	7.22 (0.8)	6.65 (0.7)	7.12 (0.8)
PPPA 1 mg/kg	10	5.78 (0.6)	6.40 (0.6)	6.54 (0.4)	6.95 (0.6)
PPPA 3 mg/kg	10	5.74 (0.6)	6.51 (0.6)	6.46 (0.4)	5.97 (0.4)
PPPA 10 mg/kg	10	5.79 (0.6)	6.02 (0.5)	7.4 (0.7)	7.24 (1.0)
Morphine 10 mg/kg	10	5.86 (0.6)	**20.00 (0.0)**	**17.64 (1.1)**	**12.42 (1.1)**

* Statistically significant difference is given in bold.

JPET Fast Forward. Published on May 25, 2006 as DOI: 10.1124/jpet.106.104737
This article has not been copyedited and formatted. The final version may differ from this version.

Table 4. Minimal effective doses, minimal ataxic doses and TI values for PPPA, CBZ and LTG

	PSN MED (mg/kg)		Rotarod MAD (mg/kg)		Therapeutic Index	
Drug	**1 hr**	**3 hr**	**1 hr**	**3 hr**	**1 hr**	**3 hr**
PPPA	3	30	>30	>30	>10	>1
CBZ	100	100	30	300	0.3	3
LTG	30	10	30	10	1	1

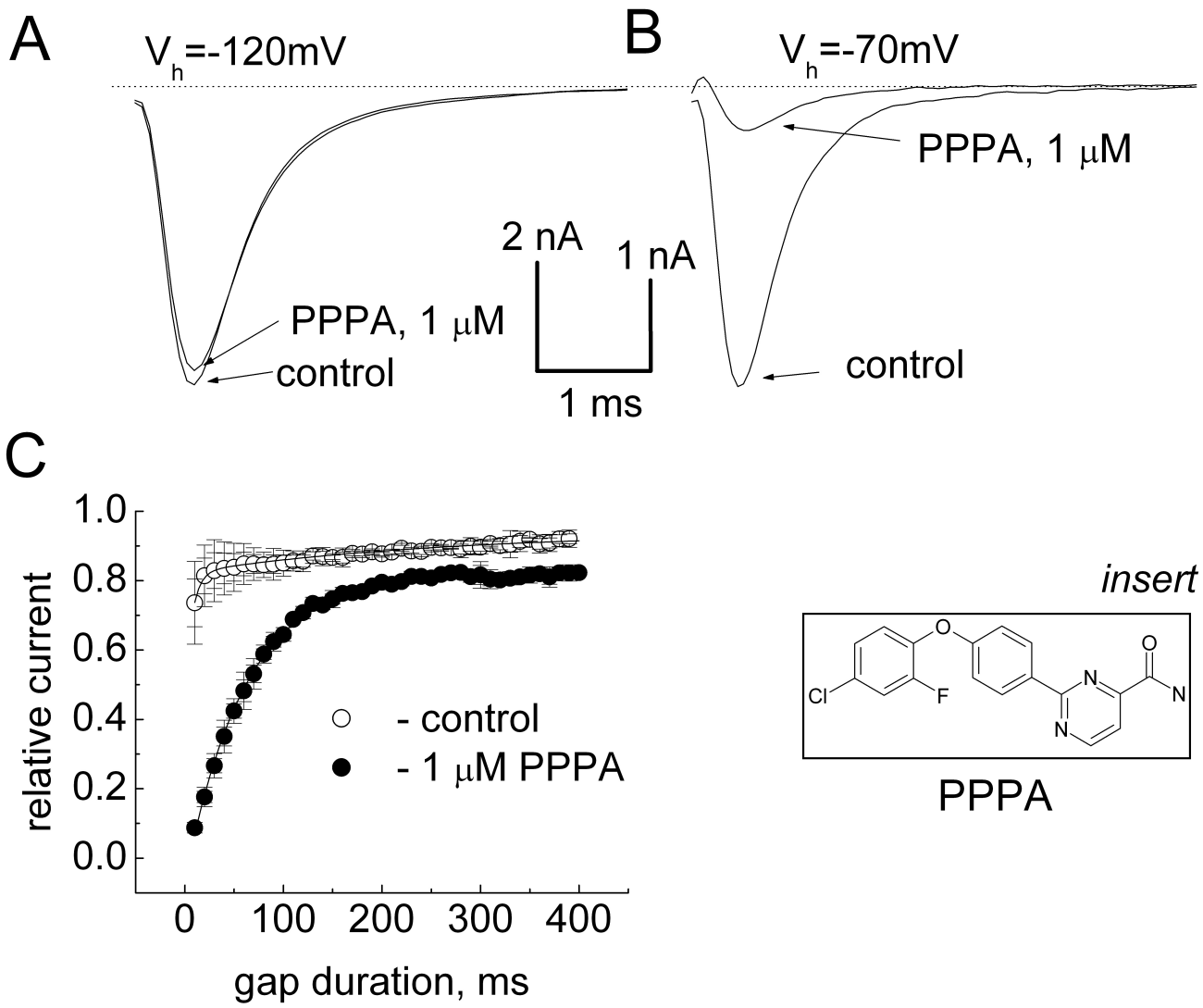

Figure 1

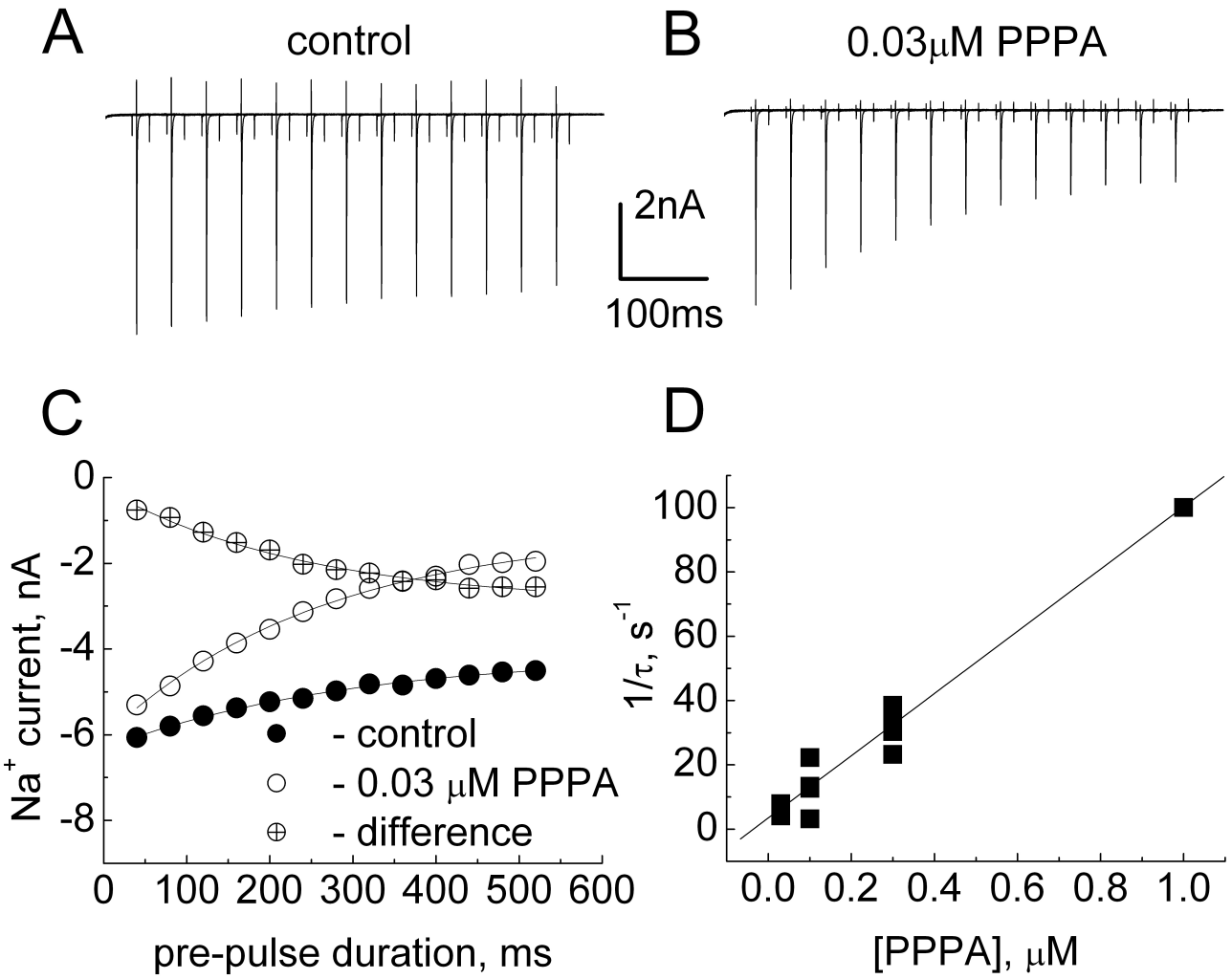

Figure 2

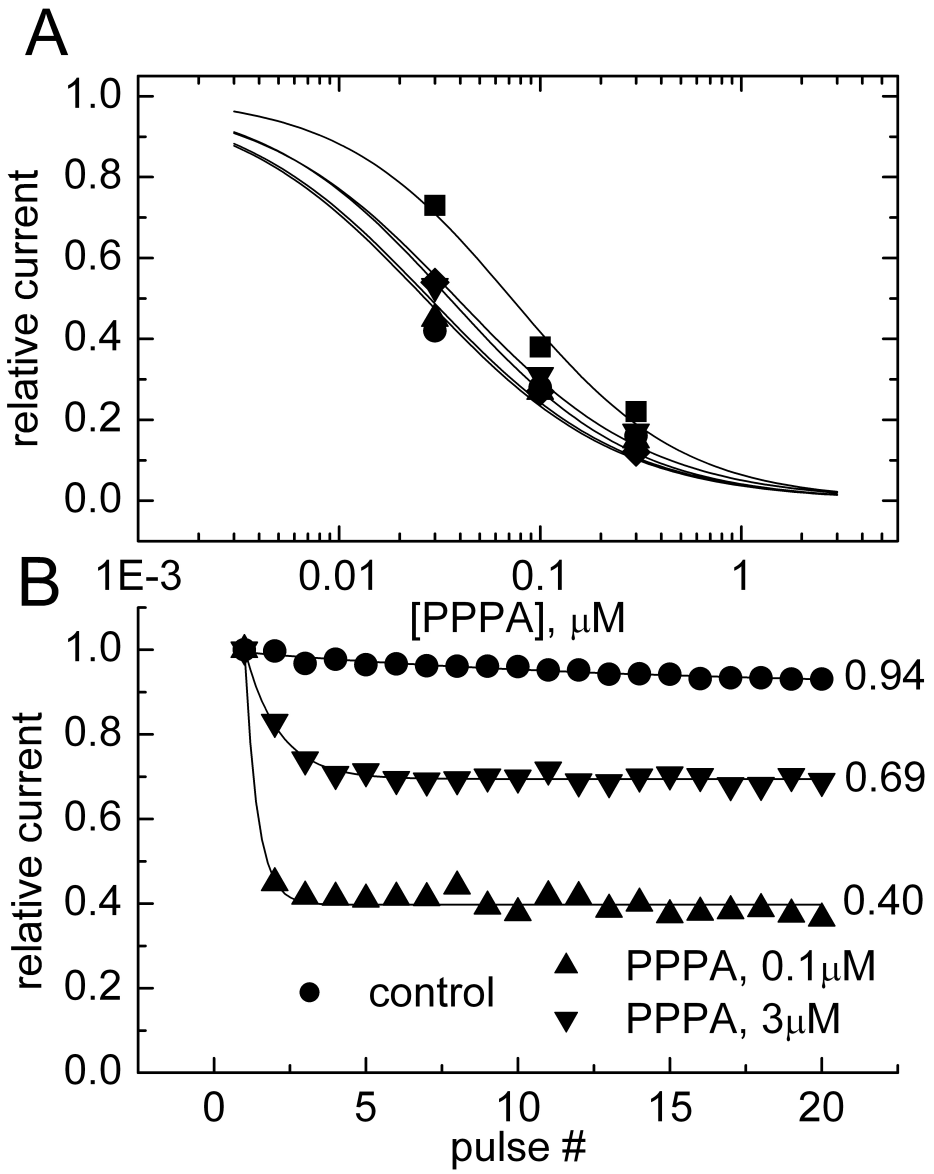

Figure 3

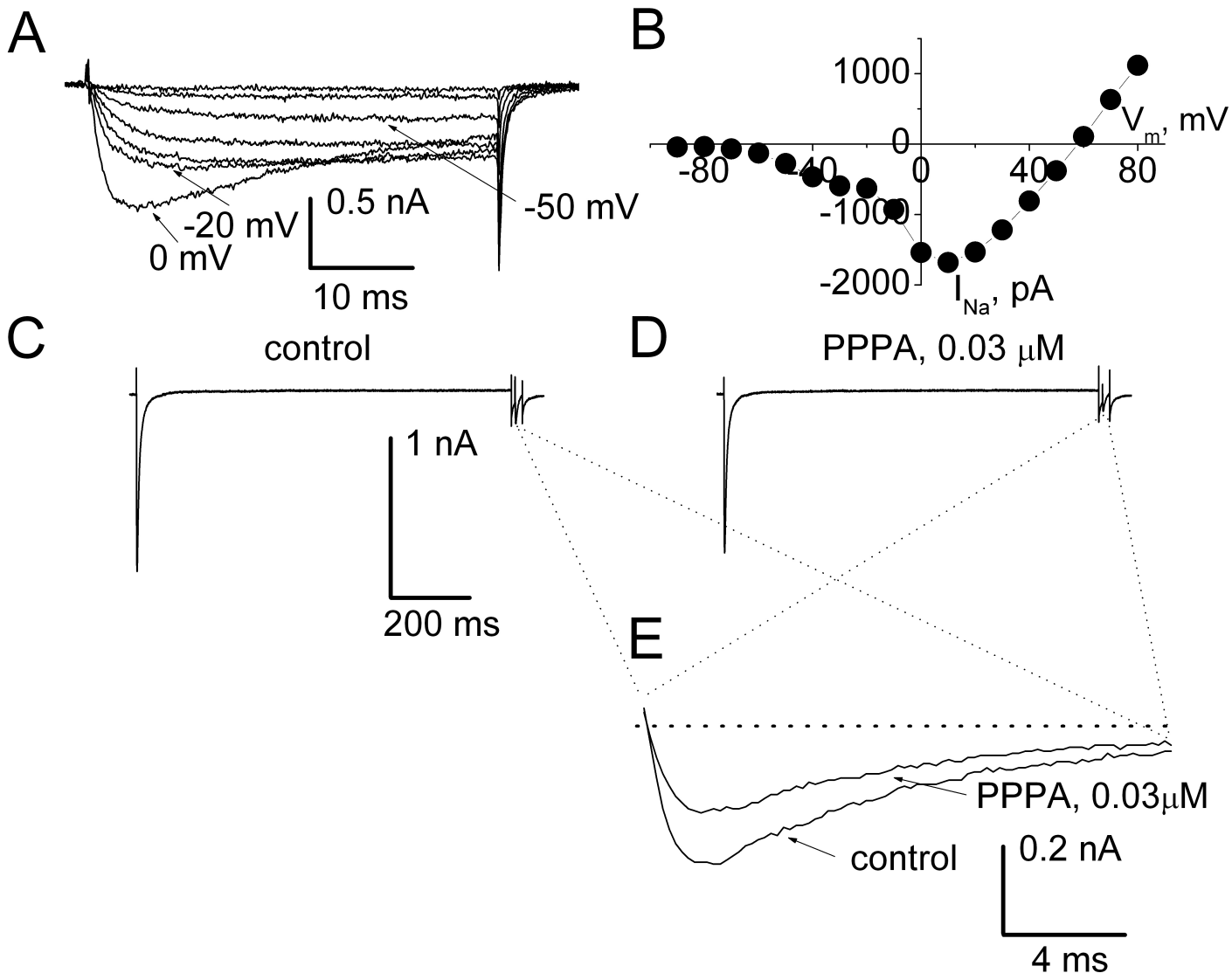

Figure 4

JPET Fast Forward. Published on May 25, 2006 as DOI: 10.1124/jpet.106.104737
This article has not been copyedited and formatted. The final version may differ from this version.